Research Article

Application of Average Differential Evolution Algorithm to Lossy Fixed Head Short-Term Hydrothermal Coordination Problem

Serdar Ozyon, Hasan Temurtas, Burhanettin Durmus, Celal Yasar

***Abstract*—Short-term hydrothermal coordination problems (STHCP) include power systems with thermal and hydraulic production units. Suppose the reservoirs of the hydraulic production units in the system are vast. In that case, it is assumed that the water in the reservoirs stays mostly the same during the operation period. Short-term hydrothermal coordination problems with hydraulic production units having this feature are called constant-head STHCP. Constant-head STHCP includes both electrical and hydraulic constraints. Variables such as the amount of water entering and leaving the reservoir of each hydraulic production unit, the reservoir capacity, and the amount of water stored in the reservoir are known as hydraulic constraints. The average differential evolution (ADE) algorithm, one of the newly developed meta-heuristic algorithms, is applied to solve the STHCP with a fixed head. Transmission line losses of the power system are calculated using the Newton-Raphson load flow method. In this study, the lossy STHCP with fixed head is solved for two cases where the input and output characteristics of the thermal generation units have both convex and non-convex characteristics. The results obtained from the solutions to both cases' problems are discussed.**

Index Terms—**Hydroelectric-thermal power generation, Newton method, Power distribution, Power generation dispatch, Evolutionary computation.**

I. INTRODUCTION

TODAY, TECHNOLOGICAL advancements in the industry demand more energy from power systems, making them more complex. In recent years, adverse conditions such as the pandemic, wars, and economic chaos have forced countries to use their existing energy resources more efficiently. Due to these unfavorable conditions and increasing energy demand, operating and planning power systems under optimum conditions has become necessary. As of the end of 2021, more than 70 percent of the world's electricity is still generated by thermal generation units using fossil fuels. As the supply of fossil fuels is gradually decreasing, the importance of efficient use of energy resources is increasing. Therefore, the current conditions necessitate the use of hydraulic resources in energy production in addition to thermal generating units [1].

The economic operation of power systems with thermal and hydraulic generation units is more complicated and complex than systems with only thermal units. Hydraulic and electrical constraints must be met in systems with hydraulic generation units. Such problems are called short-term hydrothermal coordination problems (STHCP). During the solution of STHCP, variables such as the amount of water entering and leaving the reservoirs of hydraulic units and the amount of water stored in their reservoirs are considered [2].

STHCP covers the operating period from one day to one week. In this period, it is assumed that the load profile in the system and the generation units that will feed these loads are known. The operating time considered in the problem is divided into sub-time periods, and the loads are assumed to remain constant in each period. The solution of STHCP is to find the active power generation values of all generating units, which minimizes the total fuel cost while satisfying the system's possible thermal and hydraulic constraints during the predicted operating time [2].

When we look at the studies in the literature on STHCP, two different problem structures, namely fixed and variable head, stand out. In STHCP with a fixed head, it is assumed that the amount of water in the reservoirs of hydraulic units does not change much during their operating periods. In other words, since the reservoirs are vast, the effect of net considerations on the generated active power should be addressed in solving such problems. On the other hand, in the solution of STHCP with variable head, since the reservoirs are small, the effect of the net consideration on the generated active power is taken into account [2].

In this study, the solution of the lossy STHCP with the fixed head is performed for two cases. The first case corresponds to the case where the input and output curves of the thermal generation units in the STHCP are convex, and the second case corresponds to the case where the input and

Serdar Özyön, is with Department of Electrical Engineering University of Kütahya Dumlupınar University, Kütahya, Turkey, (e-mail: serdar.ozyon@dpu.edu.tr).
https://orcid.org/0000-0002-4469-3908

Hasan Temurtaş, is with Department of Computer University of Kütahya Dumlupınar University, Kütahya, Turkey, (e-mail: hasan.temurtas@dpu.edu.tr).
https://orcid.org/0000-0001-6738-3024

Burhanettin Durmuş, is with Department of Electrical Engineering University of Kütahya Dumlupınar University, Kütahya, Turkey, (e-mail: burhanettin.durmus@dpu.edu.tr).
https://orcid.org/0000-0002-8225-3313

Celal Yaşar, is with Department of Computer Engineering University of Kütahya Health Science University, Kütahya, Turkey, (e-mail: celal_yasar@ksbu.edu.tr).
https://orcid.org/0000-0002-5069-8545

Manuscript received Mar 04, 2025; accepted Apr 21, 2025.
DOI: 10.17694/bajece.1651122

output curves are non-convex.

In the literature review, the first case, STHCP with convex fuel cost, is solved by using the Hopfield neural networks approach [3], different genetic algorithms [4-7], gravitational search algorithm [8], accelerated particle swarm optimization [9], the pseudo spot price algorithm and the gradient method [10], and mixed-integer non-linear programming [11].

In the second case, STHCP with non-convex fuel cost where valve point effects are also taken into account, simulated annealing-based goal attainment [12], non-dominated sequential genetic algorithm [13], artificial immune system search algorithm [14], cuckoo search and modified cuckoo search algorithms [15, 16] have been used in the literature, predator-prey optimization technique [17], modified dynamic neighbor learning based particle swarm optimization [18], discontinuity-based gravitational search algorithm [19] and hybrid chaotic grey wolf optimization-dragonfly algorithm [20].

This study applies the average differential evolution (ADE) algorithm, one of the newly developed metaheuristic algorithms, to solve the lossy STHCP with a fixed head. The sample test system used in the study is a system that has been previously solved in the literature, its validity has been accepted, and its results can be compared with different algorithms. The test system is based on the characteristics of a real hydrothermal power generation unit in the literature and is not directly related to a specific production unit. However, the system parameters used in the study (water inlet-outlet rates, production limits, and reservoir capacity information, etc.) have been selected by considering the theoretical general characteristics of hydrothermal power generation units. If the data of a specific production unit can be accessed, the proposed ADE algorithm can also be applied to these systems. In countries where hydrothermal power generation units are widespread, such as China, optimization studies for these systems are common, and artificial intelligence-based algorithms are frequently used. The complex structures in the systems used in these countries can be effectively optimized thanks to the high search capability of the proposed ADE algorithm. Especially in the dense energy generation areas located on the Yangtze River basin in China and connected in cascade, efficiency has been increased with production planning made with similar algorithms. The method proposed in our study has a strong potential in terms of applicability in such regions. Meta-heuristic algorithms are widely used to solve hydrothermal coordination problems to increase efficiency and continuity in worldwide energy production [21, 22].

The main contribution of this study is the application of the ADE algorithm to the lossy fixed-head STHCP, which, to the best of our knowledge, has not been previously addressed in the literature using this algorithm. To compare the performance of the ADE algorithm, the selected sample test problems were also solved by the differential evolution (DE) algorithm and gravitational search algorithm (GSA), and the results obtained were compared with each other. Newton-Raphson's AC power flow method found the transmission line losses.

Since GSA is used in reference [8] and DE is used in its classical form in reference [23] for solving STHCP in this study, the structures of these algorithms are not included in this paper. For additional information about the structures of these algorithms, the references can be consulted. The structure of ADE used to solve STHCP in this paper is described in the 'Materials and Methods' section.

II. Fixed Head Short-Term Hydrothermal Coordination Problem

In addition to minimizing the total fuel cost when solving the fixed head STHCP, it will be ensured that each hydraulic generating unit uses the desired amount of water. Hydraulic generating units are interconnected electrically (feeding the same loads) and hydraulically (such as on the same river). In this case, there can be a hydraulic serial or parallel connection between the reservoirs of the hydraulic units. Suppose two hydraulic units are located on the same river (i.e., hydraulically connected in series). In that case, the operation of the first hydraulic unit will affect the operation of the second hydraulic unit. [2, 8].

The total fuel cost (*TFC*), the objective function to be minimized in the solution of the fixed head STHCP, is given in equation (1). Since hydraulic generation units do not use any fuel other than water, the equation consists only of the fuel costs of thermal generation units [24, 25].

$$TFC = \min \sum_{j=1}^{j_{\max}} t_j \sum_{n \in N_S} F_n(P_{GS,nj}),\ (R) \tag{1}$$

In the equation, j denotes the period slots, t_j denotes the period duration, n denotes the thermal generation units, N_s denotes the set of thermal generation units, $P_{GS,n}$ denotes the active power output of n^{th} thermal generation unit, and R denotes a fictitious currency. This study considers the hourly fuel costs ($F_n(P_{GS,n})$) of thermal generation units in the fixed head STHCP in two different ways. The first one is given in equation (2) as a convex function where valve point effects are neglected, as in the first case, and the second one is given in equation (3) as a non-convex function where valve point effects are also considered, as in the second case [8, 24].

$$F_n(P_{GS,n}) = a_n + b_n.P_{GS,n} + c_n.P_{GS,n}^2,\quad (R/h),\quad n \in N_S \tag{2}$$

$$F_n(P_{GS,n}) = a_n + b_n.P_{GS,n} + c_n.P_{GS,n}^2 + \left| e_n.\sin(f_n(P_{GS,n}^{\min} - P_{GS,n})) \right|, \tag{3}$$

Convex and non-convex fuel cost functions of the thermal generation units in the system are shown together in Figure 1.

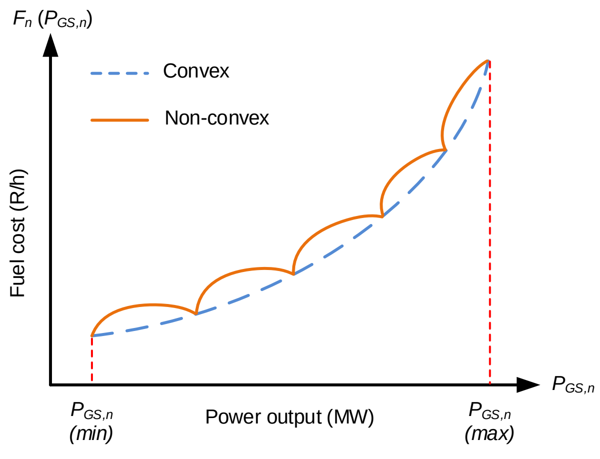

Figure 1. Input-output characteristics of thermal generation units

The input-power output curve for hydraulic generation units is shown in Figure 2. This curve shows the amount of water to be discharged per hour from the reservoir of the hydraulic unit against the active power that the hydraulic unit will generate. [24].

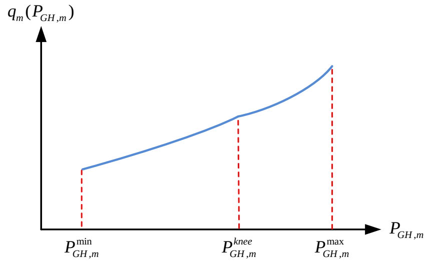

Figure 2. Input-output curve of hydraulic generation units

The amount of water discharged per hour of hydraulic generation units taken in two parts, as in Figure 2, is shown in equation (4) [7, 8, 24]. In the equation, $P_{GH,m}$ denotes the active output power of the m^{th} hydraulic generation unit, and N_H denotes the set of hydraulic generation units.

$$q_m(P_{GH,m}) = \begin{cases} d_{1,m} + d_{2,m}.P_{GH,m} & if\ P_{GH,m}^{min} \le P_{GH,m} \le P_{GH,m}^{knee} \\ d_{3,m} + d_{4,m}.P_{GH,m} + d_{5,m}.P_{GH,m}^2 & if\ P_{GH,m}^{knee} \le P_{GH,m} \le P_{GH,m}^{max} \end{cases} \quad (4)$$

Due to the nature of the hydraulic units in the system, the hydraulic relations between them can be parallel and series. If units k and l are connected in series and hydraulic unit l is after hydraulic unit k, i.e., the water discharged from hydraulic unit k enters the reservoir of hydraulic unit l, the amount of water stored in the reservoir of hydraulic unit l at the end of time j is calculated according to equation (5)

$$V_{l,j} = V_{l,j-1} - \left[q_k(P_{GH,kj}) - q_l(P_{GH,lj}) \right].t_j \quad (5)$$

The equation $V_{l,j}$ denotes the volume of water in the reservoir of hydraulic unit l^{th} at time period j^{th} and $q_k(P_{GH,kj})$ denotes the amount of water released (discharge) from hydraulic unit k^{th} at time period j. In this study, it is assumed that the water released from k^{th} hydraulic unit reaches the reservoir of l^{th} hydraulic unit without time delay. The total amount of water that the k^{th} hydraulic unit will discharge from its reservoir at the end of the $j_{max}{}^{th}$ time period is calculated from equation (6) using the input-output curve of the k^{th} unit. Similarly, the total amount of water to be consumed by the l^{th} hydraulic unit during the operating period, $q_{total,l}$, is calculated according to equation (7), depending on the reservoir start and end constraints. [8]

$$\sum_{j=1}^{j_{max}} q_k(P_{GH,kj}).t_j = q_{total,k} \quad (6)$$

$$q_{total,l} = q_{total,k} + V_l^{start} - V_l^{end} \quad (7)$$

In the equation V_l^{start} and V_l^{end} denote the initial and final water volume in the reservoir of the l^{th} hydraulic unit, respectively. The active and reactive power balance constraints in a lossy thermal and hydraulic generation unit system are shown in equations (8) and (9), respectively. In the equations, $P_{load,j}$ and $P_{loss,j}$ denotes the active load and active power loss in the j^{th} interval, while $Q_{load,j}$ and $Q_{loss,j}$ denotes the reactive load and reactive power loss in the j^{th} interval. In equation (9), $Q_{GS,nj}$ denotes the reactive output power of the n^{th} thermal production unit in the j^{th} interval, and $Q_{GH,mj}$ denotes the reactive output power of the m^{th} hydraulic production unit in the j^{th} interval [26].

$$\sum_{n\in N_S} P_{GS,nj} + \sum_{m\in N_H} P_{GH,mj} - P_{load,j} - P_{loss,j} = 0, \quad j = 1,...., j_{max} \quad (8)$$

$$\sum_{n\in N_S} Q_{GS,nj} + \sum_{m\in N_H} Q_{GH,mj} - Q_{load,j} - Q_{loss,j} = 0, \quad j = 1,...., j_{max} \quad (9)$$

In this study, active (P_{loss}) and reactive (Q_{loss}) power losses are computed using the Newton-Raphson AC power flow method. The power flow analysis is performed for each sub-time period based on the updated power generation values of the thermal and hydraulic units. This study does not use B-loss matrices to calculate transmission line losses. Instead, they are explicitly calculated for each interval using the full admittance matrix of the system and the π-equivalent models of the transmission lines. These estimated losses are then used in the power balance constraints (equations (8) and (9)), making them essential elements of the optimization process [26].

The operating limits of the thermal generation units in the system are given in equations (10) and (11), and the electrical and hydraulic constraints of the hydraulic generation units are shown in equations (12)-(16).

$$P_{GS,n}^{min} \le P_{GS,nj} \le P_{GS,n}^{max}, \quad n \in N_S, \ j = 1,\dots, j_{max} \quad (10)$$

$$Q_{GS,n}^{min} \le Q_{GS,nj} \le Q_{GS,n}^{max}, \quad n \in N_S, \ j = 1,\dots, j_{max} \quad (11)$$

$$P_{GH,m}^{min} \le P_{GH,mj} \le P_{GH,m}^{max}, \quad m \in N_H, \ j = 1,...., j_{max} \quad (12)$$

$$Q_{GH,m}^{min} \le Q_{GH,mj} \le Q_{GH,m}^{max}, \quad m \in N_H, \ j = 1,...., j_{max} \quad (13)$$

$$q_m^{min} \le q_{mj}(P_{GH,mj}) \le q_m^{max}, \quad m \in N_H, \ j = 1,...., j_{max} \quad (14)$$

$$V_m^{min} \le V_{mj} \le V_m^{max}, \quad m \in N_H, \ j = 1,...., j_{max} \quad (15)$$

$$V_{m0} = V_m^{start}, \quad V_{mj_{max}} = V_m^{end}, \quad m \in N_H \quad (16)$$

III. MATERIALS AND METHODS (AVERAGE DIFFERENTIAL EVOLUTION, ADE)

The ADE algorithm is a newly proposed metaheuristic and a new version of DE. The ADE algorithm is a method developed to improve some of the fundamental weaknesses of the DE algorithm. It is known that ADE shows faster convergence and more balanced exploration/exploitation performance thanks to its average-based mutation approach, especially in complex, highly constrained, and nonlinear problems. STCHP, which is considered in the study, is defined as a complex and nonlinear real-world engineering problem in the literature. Therefore, the ADE algorithm was preferred in line with its positive performance history in the literature and the necessity of providing a high level of accuracy and multiple constraints in this study. ADE is a population-based algorithm, and each search agent is called a solution vector. The solution vectors cooperatively attempt to find the solution vector with the best fitness-valued objective function. The evolution of solution vectors is maintained over iterations using crossover, mutation, and selection phases [27, 28].

In ADE, the initial population is first created. The possible solution candidates are randomly distributed in the search space according to equation (17).

$$\begin{aligned} & x_{i,G}^r = x_{i,\mathrm{L}} + rand.(x_{i,\mathrm{U}} - x_{i,\mathrm{L}}) \\ & i = 1,2,.....PS \quad and \quad r = 1,2,......D \end{aligned} \quad (17)$$

Where x is the solution vector set, PS is the population size, D is the number of variables in each solution, $x_{i,U}$ and $x_{i,L}$ the lower and upper bounds of the variables, $rand$ is a random number in the interval [0, 1], and $x_{i,G}^r$ is the r variable of the i^{th} individual in generation G [27, 28].

Then, the fitness values of each solution vector concerning the objective function are determined, and the candidate vector development phase begins. In this phase, candidate vector development is tested for all solution vectors in the current population. First, the mean vector for the current generation is calculated. This vector $\vec{A}_G$ is calculated as the average of all vectors in the current generation from equation (18).

$$\vec{A}_G = \frac{1}{PS}\sum_{i=1}^{PS}\vec{x}_{i,G} \tag{18}$$

Here, the vector $\vec{A}_G$ denotes the mean vector in the G generation, and the vector G denotes the solution vectors. A mutation vector for each solution is then generated from equation (19) [27, 28].

$$\vec{u}_{i,G+1} = \vec{x}_{best,G} + \gamma.rand_i[-1,1].[\vec{A}_G - \vec{x}_{i,G}] \tag{19}$$

Where $\vec{u}_{i,G+1}$ mutation vector, $\vec{x}_{best,G}$ best vector, $\vec{x}_{i,G}$ target vector, γ scaling factor and $rand_i$ random numbers are in the range [-1, 1] [27, 28].

The last step in the generation phase of the candidate solution is crossover. In this step, a parametric crossover with CR probability is performed between the mutation vector $\vec{u}_{i,G+1}$ and the target vector $\vec{x}_{i,G}$. At the end of this process, for each parameter of the solutions, a candidate vector $\hat{x}_{i,G+1}$ for the next generation is obtained from equation (20) [27, 28].

$$\hat{x}^r_{i,G+1} = \begin{Bmatrix} u^r_{i,G+1} & if \;\; rand_r[0,1] \le CR \\ x^r_{i,G} & otherwise \end{Bmatrix} \tag{20}$$

As a result, the applicability value $f\left(\hat{x}_{i,G+1}\right)$ of the candidate vector is compared with the applicability value of the target vector $f\left(\vec{x}_{i,G}\right)$. The one with a better applicability value is passed on to the next generation. The above evolutionary processes are continued through iterations. When the last iteration is reached, the computation is terminated and the solution vector with the best fit is returned as the solution. The flow chart of the algorithm is given in Figure 3 [27, 28].

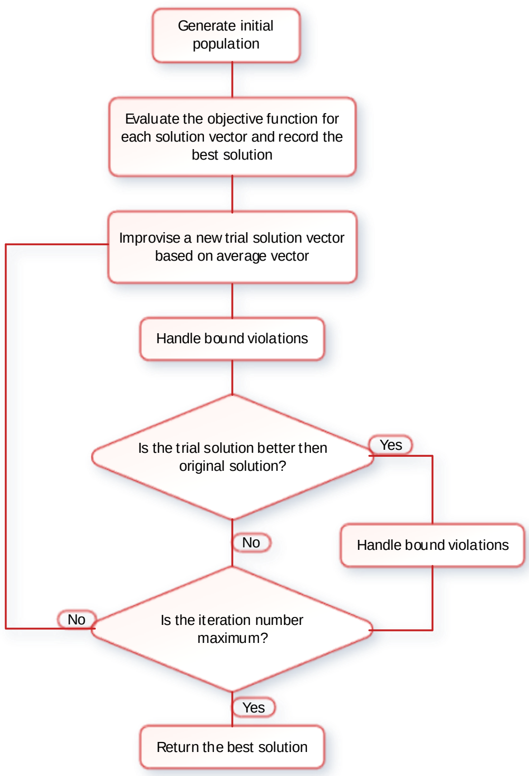

Figure 3. ADE flow chart

IV. APPLICATION OF ALGORITHMS TO PROBLEMS

To apply the algorithms considered in this study (GSA, DE, and ADE) to the STHCP with fixed head and to obtain feasible optimal solutions, the constraints given in equations (10)-(16) must be satisfied. Otherwise, the obtained solutions are not feasible optimal solutions. When starting the solution with all three algorithms (GSA, DE, and ADE), the number of individuals in the population and the number of iterations are first entered. Then, other data and parameters of each algorithm and the problem are read from the data file created. After the assignment process, the active and reactive power values of the slack bus, the power flowing from all lines, and the power losses in the system are calculated by performing the load flow for each period. Since the powers of all generation units are known, *TFC* is calculated from equation (1), and water values of hydraulic units are calculated from equations (5)-(7). It is checked whether these water values calculated by the algorithm satisfy the constraints in equations (15) and (16). If these constraints are not satisfied, a penalty function is created for each constraint that is not satisfied, and these values are added to the *TFC*. The function thus formed is called the fitness function (f). Therefore, the constraints in equations (15) and (16) are tried to be satisfied in the program with the help of the fitness function. Thus, f in Equation (24) is the objective function to obtain a feasible optimal solution instead of *TFC* in Equation (1).

$$f = TFC + TPF \tag{24}$$

The *TPF* in the equation represents the total penalty function added to make the solution conform to the constraints. Any proposed solution to the problem is penalized with the help of the penalty function when it violates the prescribed constraints. In this study, a constant penalty function approach is used. Specifically, when any defined constraints (final water volume, reservoir limits, and slack bus voltage, etc.) are violated, a constant penalty value proportional to the violation amount is added to the objective function. This approach ensures that infeasible solutions are discouraged, but not entirely discarded (i.e., a 'death penalty' is not used). The magnitude of the penalty for each constraint is controlled by the predefined penalty coefficients (CPF_{slack}, CPF_{Vend}, CPF_{Vm}), which were tuned via sensitivity analysis as explained earlier. To satisfy these constraints, the penalties are defined as the PF_{slack} slack bus, PF_{Vm} the volumes of water stored in the reservoirs of the hydraulic units, and PF_V^{end} the volumes of water remaining in the reservoirs of the hydraulic units in the last period. Therefore, the explicit form of the total *TPF* expression in equation (24) is taken as given in equation (25).

$$TPF = PF_{slack} + PF_{V_m} + PF_{V^{end}} \tag{25}$$

The details of the equations used in applying the algorithms to the STHCP problem can be obtained from [26].

V. NUMERICAL SAMPLE SOLUTION

For applying the GSA, DE, and ADE optimization algorithms to the STHCP, the sample power system, whose single-line diagram is shown in Figure 4, is selected. This sample test system was chosen because it has been previously solved in the literature with different algorithms, and acceptable solutions have been obtained. The sample test system consists of 16 buses. The system has five thermal generation units, four hydraulic generation units, and 35 transmission lines. Units connected to buses 1, 4, 5, 8, and 15 are thermal generation units, while buses 10, 12, 14, and 16 are hydraulic generation units with fixed heads. The system selects bus number one as the slack bus, whose voltage is $1.05\angle 0^0$ pu. To solve the problem, a daily operating period consisting of six equal sub-time periods of four hours each ($t_j=4h$, $j=1,...,6$) is considered. All values in the study are given according to the *pu* unit system. The test system's base values are $S_{base}=100$ *MVA*, $U_{base}=230$ *kV* and $Z_{base}=529$ *Ohm* [7, 8, 26].

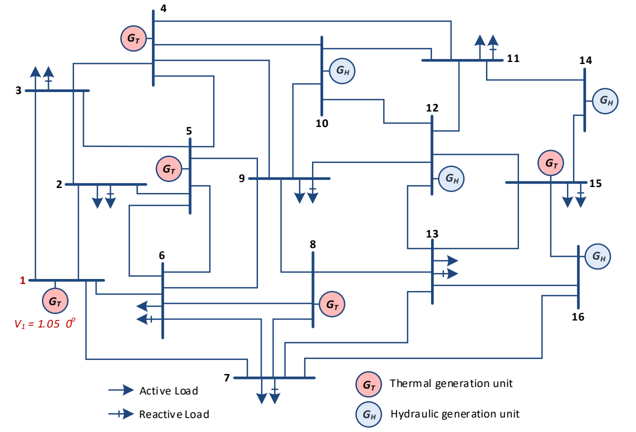

Figure 4. Single-line diagram of the system with sixteen buses and nine generators [8]

The resistance (R), reactance (X), and shunt susceptance (B) values of the nominal π equivalent circuit of the transmission lines of the sample test system, the active (P) and reactive (Q) load values for each sub-time period during the operating period, the convex fuel cost curve coefficients and power generation limits for thermal generation units and the non-convex fuel cost curve coefficients and power generation limits have been taken from references [7, 8].

The coefficients of the water input and output per hour curves of the hydraulic generating units in the test system, active power generation limits, reservoir storage limits, initial and final water volume values of the reservoirs, the amount of water per hour entering the reservoirs and the total amount of water to be discharged during the operating period are given in Table 1 [8].

TABLE I. VALUES OF HYDRAULIC PRODUCTION UNITS IN THE SYSTEM

	Hydraulic generation unit no (m)			
	10	12	14	16
d_1	330.0	320.0	380.0	300.0
d_2	497.0	620.0	565.0	600.0
d_3	254.4	275.0	432.0	343.2
d_4	200.0	380.0	200.0	228.0
d_5	300.0	180.0	250.0	280.0
$P_{GH,m}^{min}$	0.0	0.0	0.0	0.0
$P_{GH,m}^{knee}$	1.20	1.50	1.30	1.20
$P_{GH,m}^{max}$	1.35	1.65	1.45	1.35
V_m^{min}	30000	30000	30000	30000
V_m^{max}	80000	80000	80000	80000
V_m^{start}	50000	45000	46600	40000
V_m^{end}	48000	46600	40600	50600
r_{mj}	650	-	450	-
$q_{total,m}$	17600	16000	16800	22200

The units of variables $P_{GH,m}^{min}$, $P_{GH,m}^{knee}$ and $P_{GH,m}^{max}$ in the table are *pu*, and the units of water parameters required for hydraulic production are *acre-ft*.

The hydraulic relationships between the hydraulic generating units in the test system are shown in Figure 5.

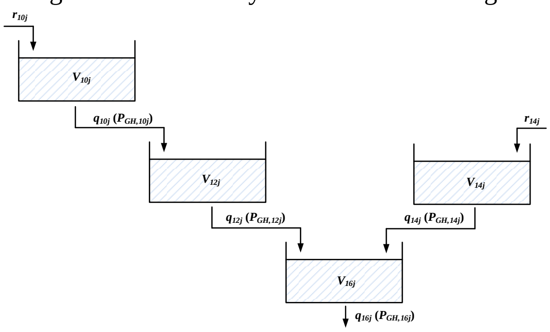

Figure 5. Hydraulic relations between hydraulic generating units

The volume of water remaining in the reservoirs of the hydraulic generating units at the end of each sub-time period is calculated from equations (26)-(29), respectively.

$$V_{10j}=V_{10j-1}+\left[r_{10}-q_{10}(P_{GH,10j})\right].t_j,\quad j=1,....,6 \tag{26}$$

$$V_{12j}=V_{12j-1}+\left[q_{10}(P_{GH,10j})-q_{12}(P_{GH,12j})\right].t_j,\quad j=1,....,6 \tag{27}$$

$$V_{14j}=V_{14j-1}+\left[r_{14}-q_{14}(P_{GH,14j})\right].t_j,\quad j=1,....,6 \tag{28}$$

$$V_{16j}=V_{16j-1}+\left[q_{12}(P_{GH,12j})+q_{14}(P_{GH,14j})-q_{16}(P_{GH,16j})\right].t_j \tag{29}$$

To be used in the Newton-Raphson load flow method applied to calculate the transmission losses of the test system, the initial reactive power values of the thermal and hydraulic generation units in the system (excluding the slack bus) in each sub-time period are given in *pu* in Table 2 [8].

TABLE II. INITIAL REACTIVE POWER VALUES AS PU OF THE GENERATION UNITS IN THE SYSTEM [8]

	Period (j)					
	1	2	3	4	5	6
4	0.400	0.550	0.600	0.700	0.650	0.500
5	0.400	0.550	0.600	0.650	0.650	0.500
8	0.400	0.550	0.600	0.600	0.600	0.500
10	0.400	0.550	0.600	0.600	0.600	0.500
12	0.400	0.550	0.600	0.700	0.600	0.500
14	0.400	0.550	0.600	0.700	0.650	0.500
15	0.400	0.550	0.600	0.700	0.600	0.500
16	0.400	0.550	0.600	0.650	0.650	0.500

All parameter values of the three algorithms (GSA, DE, and ADE) and penalty functions of the problems used to solve the STHCP with fixed head are given in Table 3.

TABLE III. PARAMETER VALUES FOR ALGORITHMS AND PROBLEMS

GSA	IteN	N	G_0	α	f_{Call}
	1000	50	100	10	50000
DE	IteN	N	CR	F	f_{Call}
	1000	50	0.9	0.5	50000
ADE	IteN	N	CR	γ	f_{Call}
	1000	50	0.9	2	50000
STHCP	$Tol_{V^{end}}$	CPF_{slack}	CPF_{V_m}	$CPF_{V^{end}}$	
	0.02	1000	0.7	0.7	

The algorithm parameters of the GSA, DE, and ADE algorithms given in Table 3 are the values used in previous studies in which the performance analyses of the parameters were made and used in solving similar problems. To ensure that constraint handling through penalty functions does not negatively impact the feasibility or quality of the solutions, a sensitivity analysis was performed on the penalty coefficients (CPF_{slack}, CPF_{Vend}, CPF_{Vm}). These coefficients were systematically varied in defined ranges (CPF_{slack}: 100-3000, CPF_{Vend}, CPF_{Vm}: 0.1-1.0), and the solutions were evaluated regarding both TFC values and constraint satisfaction. Based on these trials, the final values were set as CPF_{slack}=1000, CPF_{Vend}=0.7, and CPF_{Vm}=0.7, which provided the best balance between solution feasibility and algorithmic convergence. However, different solutions to the problem can be obtained by studying these values with other methods and approaches.

In Table 3, *IteN* indicates the number of iterations, which are the stopping criteria of the algorithms, *N* indicates the number of agents in each population, and the number of times the f_{Call} objective function is called throughout the solution. In the table, G_0 is the initial value of the GSA, α is the constant coefficient of the GSA [8], *CR* is the crossover rate of the DE, and *F* is the scaling factor of the DE algorithm [23], *CR* is the crossover rate of the ADE, and γ is the scaling factor of the ADE algorithm.

In this study, the solutions of the selected sample test systems were performed 50 times for each algorithm separately. The algorithms were developed independently in MATLAB R2021a, and the programs were run on a 2xIntel Xeon E5-2637 v4 3.50 GHz dual-processor workstation with 512 GB RAM.

A. CASE-1: STHCP WITH CONVEX THERMAL FUEL COST FUNCTION

For this case, the fuel cost function for thermal generation units in the example test system in Figure 4 is as convex as in equation (2). Using the coefficients in equation (2), the test system was solved 50 times each by GSA, DE, and ADE algorithms. First, the statistical analysis of the aggregated results obtained from these solutions is given in Table 4.

TABLE IV. VALUES FOR 50 SOLUTIONS (CASE-1)

	Solution Methods		
	GSA	DE	ADE
The best TFC (R)	149279.809206 (Run: 7)	148235.166212 (Run: 24)	147839.995227 (Run: 27)
The worst TFC (R)	153428.660945 (Run: 1)	151546.908949 (Run: 44)	152929.663208 (Run: 29)
The mean TFC (R)	151272.251286	149529.497489	149811.032659
Standard deviation	866.211041	874.248266	1237.629892
Total time (s)	13997.225157	11602.785672	12715.100654
The mean time (s)	279.944503	232.055713	254.302013

When the solution values of 50 times for this case, using the convex fuel cost functions given in Table 4, are considered, it is seen that the ADE algorithm provides a solution that meets the constraints at a lower cost than the other algorithms for the best solution value. Considering the mean cost values and times, it can be said that the DE algorithm is more stable than the other algorithms.

The graphs obtained from the solutions with all three algorithms for Case 1 are given below for comparison. For each algorithm, the logarithmic variation of the fitness functions concerning iterations is shown in Figure 6, the variation of *TFC* is shown in Figure 7, the variation of total transmission line losses (*TTLL*) in *pu* according to iterations is shown in Figure 8, and the box plots of the 50 solutions given in Table 4 are shown in Figure 9.

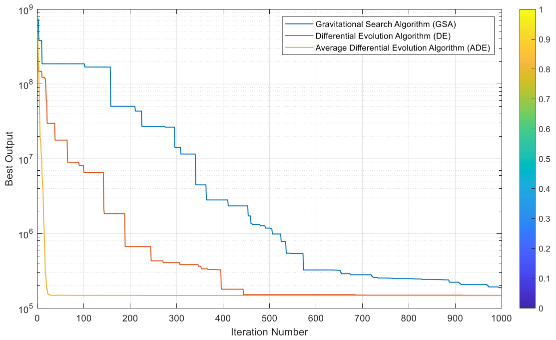

Figure 6. Variation in the fitness functions of the best solutions according to iterations (Case 1)

When the change of the fitness functions according to the algorithms given in Figure 6 is analyzed, it is seen that the ADE algorithm converges faster than the other two algorithms. In addition, when the change in *TFC* of ADE compared to the other algorithms in Figure 7 is analyzed, it can be said that it monotonically decreases continuously after the first 60th iteration and quickly reaches the optimal value by resetting the penalty functions.

The monotonically continuous decreases in the *TFC* changes of the other two algorithms start at approximately the 550th iteration in GSA and at roughly the 850th iteration in DE. Looking at the transmission line losses given in Figure 8, it can be stated that ADE, the fastest converging algorithm to the optimal value, makes minor adjustments after the 500th iteration. The other two algorithms continue to make adjustments until the last iteration. The box plots in Figure 9 show the visual dimension of the statistical values in Table 4.

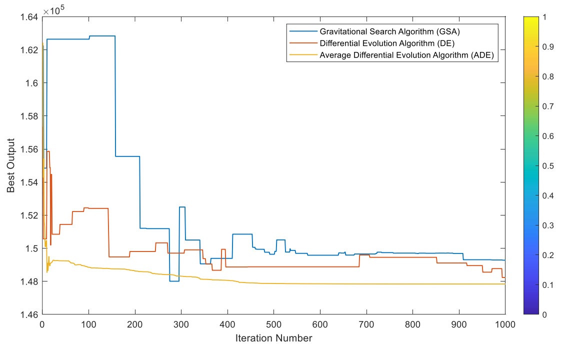

Figure 7. Variation of *TFC* of the best solutions according to iterations (Case 1)

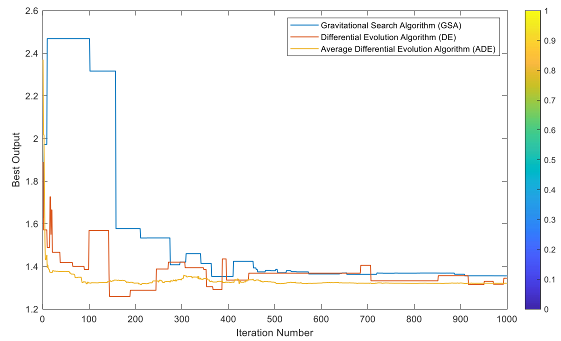

Figure 8. Variation of *TTLL* according to iterations for the example system (Case 1)

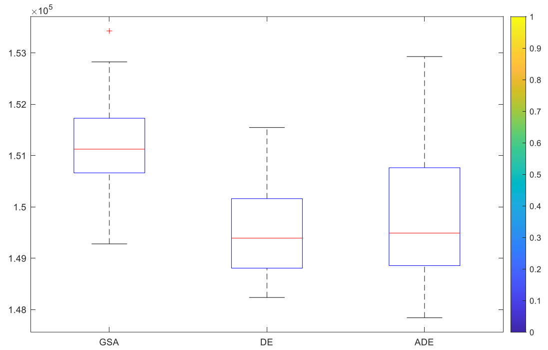

Figure 9. Box plots for 50 solutions (Case 1)

In this section, the optimal results obtained by the GSA, DE, and ADE algorithms for the solution of the sample power system are given, respectively. Firstly, the values of active and reactive power generated by the generation units, total fuel cost values (*TFC*), total transmission line losses (*TTLL*), and their durations for the run (Run: 7) where the best solution is obtained for the GSA algorithm given in Table 4 are shown in Table 5. With GSA, the best solution was obtained in run 7 with 149279.809206 *R*, and the worst solution was obtained in run 1 with 151626.969393 R. The average time for each solution was 279.944503 s, while the best solution took 280.653264 s. For the run (Run:7), where the best solution values given in the table are obtained, the variation of the active power values generated in each period is shown in Figure 10.

TABLE V. VALUES FOR THE BEST SOLUTION FOR GSA (CASE-1)

Generation unit no (n,m)		Period (j)					
		1	2	3	4	5	6
1	$P_{GS,1j}$	0.602092	1.801693	2.063385	0.332029	2.224327	0.854523
	$Q_{GS,1j}$	0.713062	0.721523	1.002791	0.901243	1.166558	0.392211
4	$P_{GS,4j}$	2.282432	0.774616	1.537482	1.196360	0.534817	0.842107
5	$P_{GS,5j}$	0.490836	1.065996	0.543045	1.932829	1.500778	1.561440
8	$P_{GS,8j}$	0.711125	1.252429	1.911400	1.289905	0.502215	0.864658
10	$P_{GH,10j}$	0.230360	1.097812	0.338926	1.177960	0.866872	1.145054
12	$P_{GH,12j}$	0.074892	0.297292	0.097467	0.966235	1.551829	0.330665
14	$P_{GH,14j}$	0.564265	0.517293	0.952478	0.727835	0.183546	0.453789
15	$P_{GS,15j}$	1.080000	0.491073	0.521613	0.867925	0.866872	1.039889
16	$P_{GH,16j}$	0.942164	1.193200	1.064607	1.175446	1.207179	0.656195
Ploss (pu)		0.178166	0.191404	0.280403	0.266524	0.288435	0.14832
TFC (R)		149279.809206					
TTLL (pu)		1.355826					
Time (s)		279.944503					

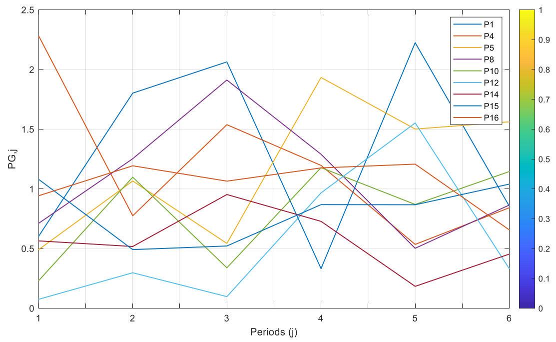

Figure 10. Variation of the values of active power generated in each period (GSA - Case 1)

The water volume values in the reservoirs at the end of the sub-periods and the error rates within acceptable limits for the solution in the 7th study, which has the best total fuel cost among the 50 solutions made with GSA, are given in Table 6. The $V_m^{end,solution}$ value in the table represents the calculated value of the volume of water remaining in the reservoir of the m^{th} hydraulic unit in the last period in the optimal solution of the test problem.

TABLE VI. RESERVOIR WATER VALUES OF THE BEST SOLUTION OBTAINED WITH GSA (CASE 1)

	Reservoir water amount (acre-ft)			
	V_{10}	V_{12}	V_{14}	V_{16}
V_{start}	50000	45000	46600	40000
$V_m^{end,solution}$	48019.192239	46607.093781	40597.795222	50594.163206
V_{end}	48000	46600	40600	50600
%ErrorV	0.039984	0.015223	0.005430	0.011535
%TotalErrorV	0.0722			

Secondly, the values of active and reactive power generated by the generation units, total fuel cost values (*TFC*), total transmission line losses (*TTLL*), and durations of the run (Run: 24) where the best solution is obtained for the DE algorithm given in Table 4 are shown in Table 7.

TABLE VII. VALUES FOR THE BEST SOLUTION FOR DE (CASE-1)

Generation unit no (n,m)		Period (j)					
		1	2	3	4	5	6
1	$P_{GS,1j}$	2.191521	2.068250	1.593236	1.368718	2.822614	1.720313
	$Q_{GS,1j}$	0.771368	0.755874	0.755874	1.019166	1.314003	0.467084
4	$P_{GS,4j}$	0.549319	0.538031	1.120449	1.770410	1.570902	0.524182
5	$P_{GS,5j}$	1.241671	0.400000	1.233339	0.687416	1.186104	1.022992
8	$P_{GS,8j}$	0.500000	1.356888	1.239920	0.842645	0.874138	0.811322
10	$P_{GH,10j}$	0.538195	1.094782	0.873570	1.029616	0.545843	0.786761
12	$P_{GH,12j}$	0.123876	0.137408	0.927461	0.548743	0.944911	0.671698
14	$P_{GH,14j}$	0.256920	0.909208	0.389392	1.117681	0.177734	0.547895
15	$P_{GS,15j}$	0.565038	0.741216	0.504363	1.229466	0.527297	0.699885
16	$P_{GH,16j}$	0.987006	1.253919	1.115424	1.090656	0.802402	0.971872
Ploss (pu)		0.153546	0.199702	0.247154	0.285351	0.301945	0.15692
TFC (R)		148235.166212					
TTLL (pu)		1.344620					
Time (s)		228.469464					

For the run (Run: 24), where the numerical values given in the table are obtained, the variation of the active power values generated in each period is shown in Figure 11.

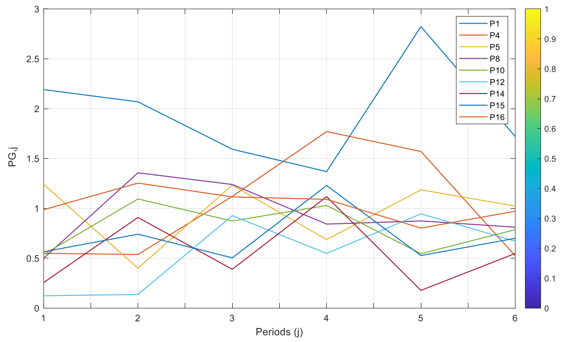

Figure 11. Variation of the values of active power generated in each period (DE - Case 1)

The best solution with DE occurred in run 24 with 148235.166212 *R*, and the worst solution occurred in run 44 with 151546.908949 *R*. The average time for each solution was 232.055713 s, while the best solution, 24, took 228.469464 s. The water volume values and error rates in the reservoir at the end of the sub-time periods for the solution in the 24th study, which has the best total fuel cost among the 50 solutions made with DE, are given in Table 8. Thirdly, the active and reactive power values, total fuel cost values (*TFC*), total transmission line losses (*TTLL*), and durations for the study (Run: 27) where the best solution is obtained for the ADE algorithm given in Table 4 are shown in Table 9.

Out of the 50 solutions obtained with the ADE algorithm, the best fuel cost solution was obtained in run 27 with 147839.995227 *R*, and the worst solution was obtained in run 29 with 152929.663208 *R*. The average time for each solution was 254.302013 seconds, while the best solution in run 27 took 244.675648 seconds.

TABLE VIII. RESERVOIR WATER VALUES OF THE BEST SOLUTION OBTAINED WITH DE (CASE 1)

	Reservoir water amount (acre-ft)			
	V_{10}	V_{12}	V_{14}	V_{16}
V_{start}	50000	45000	46600	40000
$V_m^{end,solution}$	48000.889136	46600.949646	40598.645451	50600.487163
V_{end}	48000	46600	40600	50600
%ErrorV	0.001852	0.002038	0.003336	0.000963
%TotalErrorV	0.0082			

For the run (Run: 27), where the numerical values given in the table are obtained, the variation of the active power values generated in each period is shown in Figure 12.

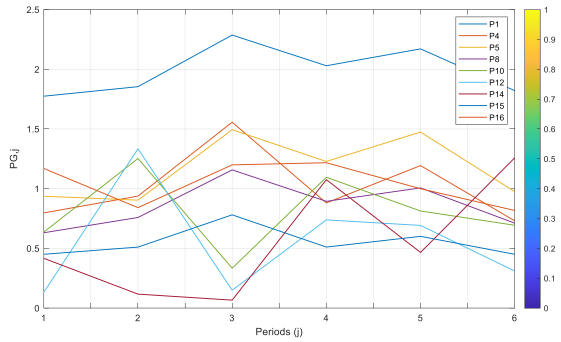

Figure 12. Variation of the values of active power generated in each period (ADE - Case 1)

TABLE IX. VALUES OF THE BEST SOLUTION FOR ADE (CASE-1)

Generation unit no (n,m)		Period (j)					
		1	2	3	4	5	6
1	$P_{GS,1j}$	1.774286	1.854101	2.286389	2.029399	2.170580	1.820789
	$Q_{GS,1j}$	0.694538	0.727651	1.023229	1.033674	1.125214	0.538163
4	$P_{GS,4j}$	0.796903	0.937555	1.556399	0.880511	1.193176	0.730586
5	$P_{GS,5j}$	0.936526	0.903555	1.493806	1.227610	1.474010	0.974627
8	$P_{GS,8j}$	0.630608	0.758486	1.157036	0.893858	1.006261	0.710798
10	$P_{GH,10j}$	0.636121	1.252304	0.333587	1.095247	0.813018	0.693263
12	$P_{GH,12j}$	0.131896	1.333722	0.149566	0.738431	0.692042	0.309951
14	$P_{GH,14j}$	0.416561	0.116569	0.066265	1.075311	0.465786	1.258104
15	$P_{GS,15j}$	0.450193	0.510470	0.780742	0.510678	0.600481	0.450132
16	$P_{GH,16j}$	1.169090	0.840846	1.199116	1.217093	0.999479	0.817257
Ploss (pu)		0.142184	0.207608	0.272906	0.268138	0.264833	0.165507
TFC (R)		147839.995227					
TTLL (pu)		1.321178					
Time (s)		244.675648					

For Case 1, the comparison of the results obtained in this study in terms of total fuel cost (TFC) with the results of different meta-heuristic algorithms previously published in the literature is given in Table 10.

TABLE X. LITERATURE COMPARISON (CASE 1)

	GA [10]	GSA	DE	ADE
TFC (R)	148767.660	149279.809	148235.166	147839.995

The table shows that the best solution is obtained with the ADE algorithm. The comparisons in the table were made over fuel costs regardless of the amount of water discharged or not discharged by the hydraulic units in the system. The comparisons in the table were made over fuel costs irrespective of the amount of water discharged or not discharged by the hydraulic units in the system. The water volume values and error rates in the reservoir at the end of the sub-time periods for the solution in the 27th study, which has the best total fuel cost among the 50 solutions made with ADE, are given in Table 11.

B. CASE-2: STHCP WITH NON-CONVEX THERMAL FUEL COST FUNCTION

This case is designed to contribute a sample test problem for non-convex lossy STHCP with fixed head to the literature. Because the B matrix is usually used in the literature to solve such problems, however, as shown in Figure 4, the losses of the example power system can be solved with load flow when the states of the generation units at the buses, loads, and R, X, and *B* values of the transmission lines are known. Therefore, in this case, to contribute to the literature, the non-convex fuel cost functions of Figure 4 are taken as in equation (3). The values are used for the coefficients in equation (3), and this problem is solved 50 times each by GSA, DE, and ADE algorithms, respectively. First, the statistical analysis of the aggregated results obtained from the solutions of the three different algorithms is given in Table 12.

TABLE XI. RESERVOIR WATER VALUES OF THE BEST SOLUTION OBTAINED WITH ADE (CASE 1)

	Reservoir water amount (acre-ft)			
	V_{10}	V_{12}	V_{14}	V_{16}
V_{start}	50000	45000	46600	40000
$V_m^{end,solution}$	47999.020605	46599.072418	40599.173708	50598.980142
V_{end}	48000	46600	40600	50600
%ErrorV	0.002040	0.001991	0.002035	0.002016
%TotalErrorV	0.0081			

TABLE XII. VALUES FOR 50 SOLUTIONS (CASE 2)

	Solution Methods		
	GSA	DE	ADE
The best TFC (R)	177414.249557 (Run: 2)	171627.154727 (Run: 47)	156316.715581 (Run: 47)
The worst TFC (R)	193928.660732 (Run: 50)	195154.228166 (Run: 4)	175161.020942 (Run: 46)
The mean TFC (R)	187202.809936	181854.837533	163483.43463
Standard deviation	3832.031012	5006.662745	4700.180592
Total time (s)	13949.699205	11402.936344	12946.616234
The mean time (s)	278.993984	228.058727	258.932325

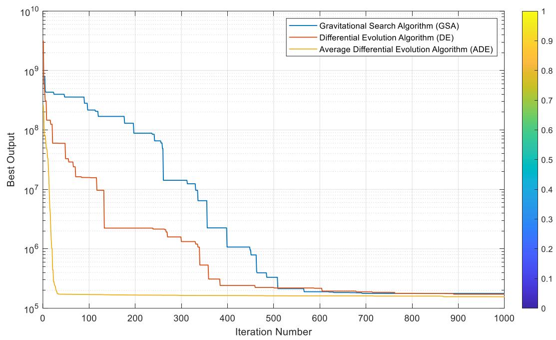

Figure 13. Variation of the fitness functions of the best solutions according to iterations (Case 2)

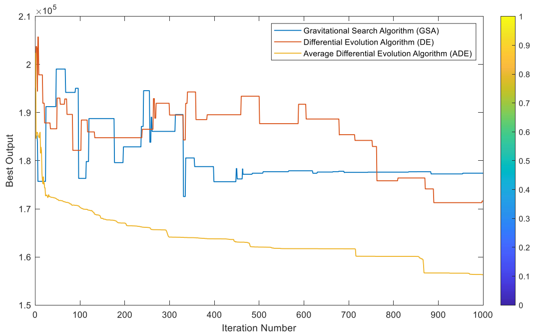

Figure 14. Variation of *TFC* of the best solutions according to iterations (Case 2)

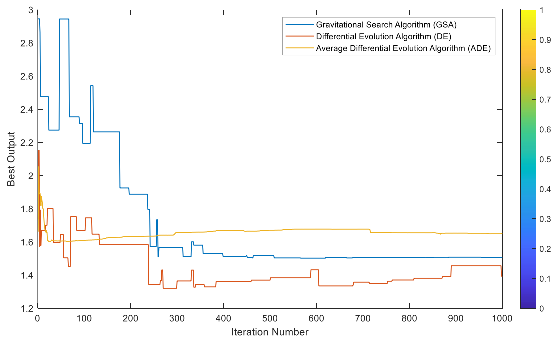

Figure 15. Variation of total transmission line losses (*TTLL*) according to iterations for the example system (Case 2)

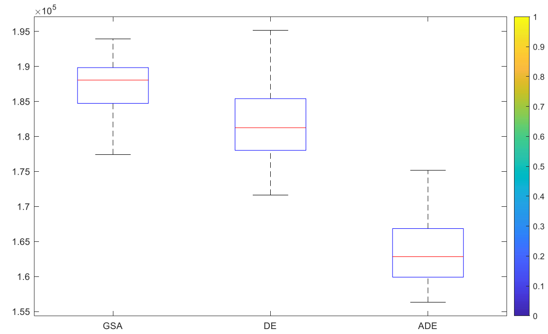

Figure 16. Box plots for 50 solutions (Case 2)

Table 12 shows that the ADE algorithm is remarkably superior to the other algorithms for the best, worst, and mean solution values when the solution values are analyzed 50 times each for this case, where non-convex fuel cost functions are used. Valve point effects are also taken into account. Considering the solution times, the DE algorithm provides an acceptable solution proposal in a shorter time than the other algorithms. For case 2, the graphs obtained for the solutions with all three algorithms are given below for comparison. For each algorithm, the logarithmic variation of the fitness functions concerning iteration is shown in Figure 13, the variation of *TFC* is shown in Figure 14, the variation of total transmission line losses (*TTLL*) in *pu* is shown in Figure 15, and the box plots of the 50 solutions given in table 15 are shown in Figure 16.

When the change of the fitness functions according to the algorithms given in Figure 13 is analyzed, it is seen that the ADE algorithm converges faster than the other two algorithms in this case as well. Also, when the change in *TFC* of ADE compared to the other algorithms is analyzed in Figure 14, it can be said that it monotonically decreases continuously after the first 20th iterations and reaches the optimum value by resetting the penalty functions at the 870th iteration. The monotonically continuous decreases in the *TFC* changes of the other two algorithms occur only after approximately the 900th iteration. Looking at the transmission line losses given in Figure 15, it can be seen that ADE, again, the algorithm that converges fastest to the optimal value, makes minor adjustments after the 700th iteration. On the other hand, of the other two algorithms, GSA converges at about the 630th iteration, whereas DE continues to make adjustments until the last iteration. The box plots in Figure 16 show the visualization of the statistical values in Table 12, and it can be stated that ADE captures the best values.

In this section, the optimal results obtained by the GSA, DE, and ADE algorithms for the solution of the non-convex fuel cost example test system, where valve point effects are also considered, are given respectively. Firstly, the values of active and reactive power generated by the generation units, total fuel cost values (*TFC*), total transmission line losses (*TTLL*), and durations for the run (Run: 2) where the best solution is obtained for GSA are given in Table 13.

TABLE XIII. VALUES FOR THE BEST SOLUTION FOR GSA (CASE 2)

Generation unit no (n,m)		Period (j)					
		1	2	3	4	5	6
1	$P_{GS,1j}$	0.427296	0.323931	2.242475	1.792951	0.328232	0.543327
	$Q_{GS,1j}$	0.613009	0.756310	1.145564	1.030746	1.207636	0.566284
4	$P_{GS,4j}$	1.039219	0.671167	2.400021	1.739655	0.573841	2.500000
5	$P_{GS,5j}$	1.625803	0.520303	0.590747	1.206818	1.840584	0.632617
8	$P_{GS,8j}$	1.367482	1.728999	0.523720	1.364441	0.774934	0.731281
10	$P_{GH,10j}$	0.462019	0.493085	1.022084	0.669538	1.270047	0.889547
12	$P_{GH,12j}$	0.098420	1.578938	0.010959	0.324641	0.748655	0.552449
14	$P_{GH,14j}$	0.313522	1.311731	0.962809	0.176430	0.283474	0.344727
15	$P_{GS,15j}$	0.474695	1.100372	0.621935	1.059844	2.316393	0.837272
16	$P_{GH,16j}$	1.131955	0.815768	0.694223	1.329163	1.349343	0.771285
Ploss (pu)		0.140411	0.244294	0.318973	0.263481	0.335503	0.202505
TFC (R)		177414.249557					
TTLL (pu)		1.505169					
Time (s)		289.714972					

TABLE XIV. VALUES FOR THE BEST SOLUTION FOR DE (CASE-2)

Generation unit no (n,m)		Period (j)					
		1	2	3	4	5	6
1	$P_{GS,1j}$	0.804705	1.997618	2.020782	2.383630	2.983880	0.537479
	$Q_{GS,1j}$	0.651131	0.725297	0.936389	1.048838	1.345280	0.487256
4	$P_{GS,4j}$	1.755174	0.903577	0.503391	0.581640	1.485320	0.513693
5	$P_{GS,5j}$	0.419269	0.480630	1.087418	0.400000	0.460585	0.939872
8	$P_{GS,8j}$	0.500000	1.681917	1.796214	1.713031	0.529823	2.000000
10	$P_{GH,10j}$	0.692746	0.556634	0.977754	0.893860	0.822674	0.927008
12	$P_{GH,12j}$	0.398535	0.082468	0.491910	1.337532	0.404853	0.640892
14	$P_{GH,14j}$	0.335638	0.853500	0.309287	0.794631	0.395915	0.708327
15	$P_{GS,15j}$	1.111508	0.918296	0.547912	1.039262	1.075420	0.450000
16	$P_{GH,16j}$	0.944397	1.016227	1.281899	0.536860	1.306330	1.061765
Ploss (pu)		0.161972	0.190867	0.266567	0.280446	0.3148	0.179036
TFC (R)		171627.154727					
TTLL (pu)		1.393689					
Time (s)		218.800278					

For Case 2, the best solution with GSA was obtained in run 2 with 177414.249557 *R*, and the worst solution was obtained in run 50 with 193928.660732 *R*. The mean time for each solution was 278.993984 seconds, while the best solution took 289.714972 seconds. For the run (Run:2), where the best solution values given in the table are obtained, the variation of the active power values generated in each period is shown in Figure 17.

Secondly, for Case 2, the values of active and reactive power generated by the generation units, total fuel cost values (*TFC*), total transmission line losses (*TTLL*), and durations for the run (Run: 47) where the best solution is obtained for the DE algorithm are given in Table 14.

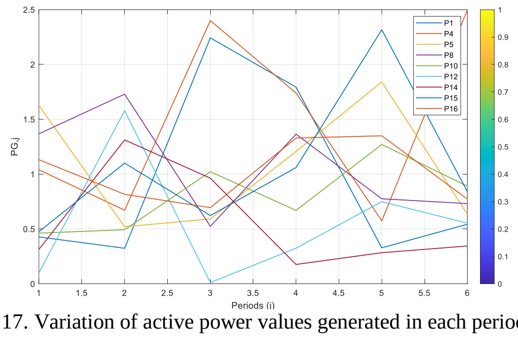

Figure 17. Variation of active power values generated in each period (GSA - Case 2)

The water volume values in the reservoirs at the end of the sub-time periods of the solution with the best total fuel cost among the 50 solutions made with GSA, and the error rates within acceptable limits are given in Table 15.

For case 2, the best solution with DE occurred in run 47 with 171627.154727 *R*, and the worst was in run 4 with 195154.228166 *R*. The mean time for each solution was 228.058727 s, while the best solution, 47, took 218.800278 s. The water volume values and error rates in the reservoir at the end of the sub-time periods for the solution in the 47th run, which has the best total fuel cost among the 50 solutions with DE, are given in Table 16.

TABLE XV. RESERVOIR WATER VALUES OF THE BEST SOLUTION OBTAINED WITH GSA (CASE 2)

	Reservoir water amount (acre-ft)			
	V_{10}	V_{12}	V_{14}	V_{16}
V_{start}	5000	45000	46600	40000
$V_m^{end,solution}$	48000.626009	46601.291171	40598.999362	50601.038430
V_{end}	48000	46600	40600	50600
%ErrorV	0.001304	0.002771	0.002465	0.002052
%TotalErrorV	0.0086			

For the study in which the numerical values given in Table 15 were obtained (Run: 47), the variation of the active power values generated in each period is shown in Figure 18.

Out of the 50 solutions obtained with the ADE algorithm, the solution with the best fuel cost value was obtained in run 47 with 156316.715581 *R*, and the worst solution was obtained in run 46 with 175161.020942 *R*. The mean time for each solution was 258.932325 s, while the best solution in run 47 took 265.273997 s.

For the run where the numerical values given in the table are obtained (Run: 47), the variation of the active power values generated in each period is shown in Figure 19.

Thirdly, the active and reactive power values, total fuel cost values (*TFC*), total transmission line losses (*TTLL*), and durations produced by the generation units belonging to the run (Run: 47) in which the best solution is obtained for the *ADE* algorithm given in Table 17.

TABLE XVI. RESERVOIR WATER VALUES OF THE BEST SOLUTION OBTAINED WITH DE (CASE 2)

	Reservoir water amount (acre-ft)			
	V_{10}	V_{12}	V_{14}	V_{16}
V_{start}	50000	45000	46600	40000
$V_m^{end,solution}$	47997.095585	46599.555628	40602.106815	50601.246730
V_{end}	48000	46600	40600	50600
%ErrorV	0.006051	0.000954	0.005189	0.002464
%TotalErrorV	0.0147			

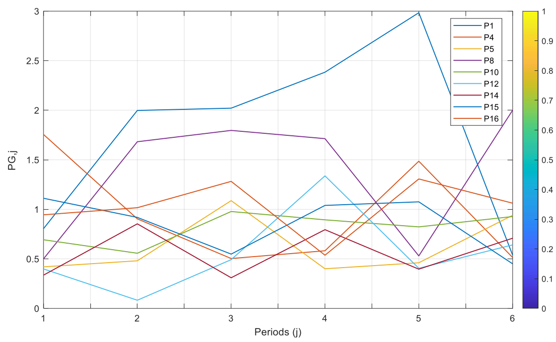

Figure 18. Variation of active power values generated in each period (DE - Case 2)

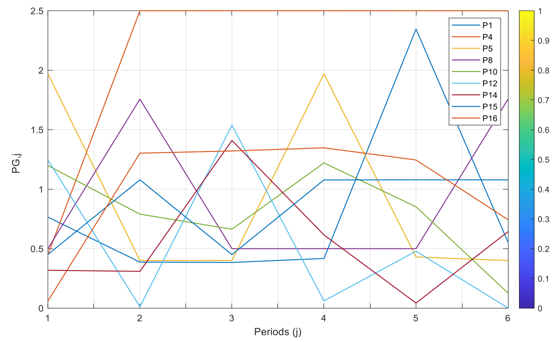

Figure 19. Variation of active power values generated in each period (ADE - Case 2)

TABLE XVII. VALUES OF THE BEST SOLUTION FOR ADE (CASE-2)

Generation unit no (n,m)		Period (j)					
		1	2	3	4	5	6
1	$P_{GS,1j}$	0.765391	0.387043	0.384259	0.417756	2.345753	0.553943
	$Q_{GS,1j}$	0.656796	0.789343	1.303577	1.146303	1.352644	0.588291
4	$P_{GS,4j}$	0.450000	2.499846	2.500000	2.500000	2.499962	2.499494
5	$P_{GS,5j}$	1.970791	0.400169	0.400052	1.969904	0.430456	0.400003
8	$P_{GS,8j}$	0.500019	1.756696	0.500028	0.500195	0.50000	1.756686
10	$P_{GH,10j}$	1.198536	0.789944	0.663727	1.220638	0.852020	0.127014
12	$P_{GH,12j}$	1.245557	0.011604	1.538311	0.061015	0.478980	0.000950
14	$P_{GH,14j}$	0.318356	0.309334	1.409196	0.615241	0.042858	0.643276
15	$P_{GS,15j}$	0.451172	1.078534	0.450091	1.077901	1.078717	1.078377
16	$P_{GH,16j}$	0.059350	1.302802	1.321014	1.347606	1.245407	0.743823
Ploss (pu)		0.159172	0.235972	0.416678	0.310256	0.324153	0.203566
TFC (R)		156316.715581					
TTLL (pu)		1.649799					
Time (s)		265.273997					

The water volume values and error rates in the reservoir at the end of the sub-time periods for the solution in the 47th run, which has the best total fuel cost among the 50 solutions with DE, are given in Table 18.

TABLE XVIII. RESERVOIR WATER VALUES OF THE BEST SOLUTION OBTAINED WITH ADE (CASE-2)

	Reservoir water amount (acre-ft)			
	V_{10}	V_{12}	V_{14}	V_{16}
V_{start}	50000	45000	46600	40000
$V_m^{end,solution}$	47999.033619	46599.619931	40599.122758	50599.072088
V_{end}	48000	46600	40600	50600
%ErrorV	0.002013	0.000816	0.002161	0.001834
%TotalErrorV	0.0068			

The comparison of the results obtained in this study for Case 2 with the results of different heuristic algorithms previously published in the literature is given in Table 19.

When the table is examined, it is seen that the ADE algorithm achieved the best result with *156316.715 R* in terms of TFC. The comparisons in the table are based on total fuel costs regardless of the amount of water discharged or not discharged by the hydraulic units in the system. The comparisons are made for acceptable tolerance values for the feasible solution to the problem in all studies.

TABLE XIX. LITERATURE COMPARISON (CASE-2)

	IGSA-1 [26]	**IGSA-2 [26]**	**IGSA-3 [26]**
TFC (R)	166516.440	165259.461	164762.279
	GSA	**DE**	**ADE**
	177414.249	171627.154	156316.715

VI. RESULTS AND CONCLUSION

To our knowledge, ADE, one of the newly developed meta-heuristic algorithms for solving STHCP with a constant drop, is applied for the first time in this study for two cases (convex and non-convex cases). The same problems are solved with both GSA and DE metaheuristics to evaluate the performance of ADE on fundamental issues. For each case, the results obtained from the solutions of the three algorithms (GSA, DE, and ADE) are compared with the values in the literature and with each other.

For the optimal solution of the fixed head STHCP, transmission line losses are calculated using the Newton-Raphson load flow method in three meta-heuristic algorithms (GSA, DE, and ADE). The study solved problems 50 times each with all three algorithms. The best TFC values in the solution of the example test system in Case 1 were 149342.548 R for GSA, 148184.488 R for DE, and 147743.228 R for ADE. ADE, which was applied to this type of problem for the first time, achieved a better result of approximately 441.26 R than the classical DE in terms of TFC values. When compared in terms of solution times, the ADE algorithm reached the solution in shorter times than the GSA and DE algorithms. Similarly, the best TFC values in the solution of the example test system in Case 2 were obtained as 177414.249 R for GSA, 171627.154 R for DE, and 156316.715 R for ADE. In this problem, when compared to TFC values, ADE achieved a better result than classical DE. However, the DE algorithm solved the issue faster than the solution times. In the optimal solutions of GSA, DE, and ADE algorithms for both cases in the study, the amount of water required to be spent by the hydraulic production units of the test systems was within the maximum error tolerance value of 0.2%.

The penalty function method is adopted in this study. That is, penalty functions provide the problem's constraints in the algorithms. In the optimal solution, this method causes an increase in the number of iterations depending on the number of constraints and thus increases the solution time. This is the disadvantage of the penalty method.

In this study, it has been successfully demonstrated that the STHCP with a lossy fixed head, which is one of the optimization problems with many constraints that has a considerable place in the literature and is of great importance in electrical engineering, can be solved with ADE, one of the newly developed meta-heuristic algorithms.

ACKNOWLEDGMENT

This research has been supported by Kütahya Dumlupınar University Scientific Research Projects Coordination Office under grant number #2021-09.

We would also like to thank Kütahya Dumlupınar University Intelligent Systems Design Application and Research Center (ASTAM) for providing some basic research facilities.

CONFLICT OF INTEREST

The authors declare that the research was conducted without any commercial or financial relationships that could be construed as a potential conflict of interest.

PUBLISHER'S NOTE

REFERENCES

[1] S. A. Papazis, G. C. Bakos, "Generalized Model of Economic Dispatch Optimization as an Educational Tool for Management of Energy Systems," Advances in Electrical and Computer Engineering, vol.21, no.2, pp.75-86, 2021. doi:10.4316/aece.2021.02009

[2] C. Yaşar, S. Özyön, "A Modified Incremental Gravitational Search Algorithm for Short-Term Hydrothermal Scheduling with Variable Head," Engineering Applications of Artificial Intelligence, vol.95 (103845), pp.1-17, 2020. doi:10.1016/j.engappai.2020.103845

[3] M. Basu, "Hopfield Neural Networks for Optimal Scheduling of Fixed Head Hydrothermal Power Systems," Electric Power Systems Research, vol.64, no.1, pp.11-15, 2023. doi:10.1016/S0378-7796(02)00118-9

[4] C. E. Zoumas, A. G. Bakirtzis, J. B. Theocharis, V. Petridis, "A Genetic Algorithm Solution Approach to the Hydrothermal Coordination Problem," IEEE Transactions on Power Systems, vol.19, no.2, pp.1356-1364, 2004. doi:10.1109/TPWRS.2004.825896

[5] J. Sasikala, M. Ramaswamy, "Optimal Gamma based Fixed Head Hydrothermal Scheduling using Genetic Algorithm," Expert Systems with Applications, vol.37, no.4, pp.3352-3357, 2009. doi:10.1016/j.eswa.2009.10.015

[6] V. S. Kumar, M. R. Mohan, "A Genetic Algorithm Solution to the Optimal Short-term Hydrothermal Scheduling," International Journal of Electrical Power & Energy Systems, vol.33, no.4, pp.827-835, 2010. doi:10.1016/j.ijepes.2010.11.008

[7] S. Özyön, C. Yaşar, Y. Aslan, H. Temurtaş, "Solution to Environmental Economic Power Dispatch Problems in Hydrothermal Power Systems by Using Genetic Algorithm," in 6th International Conference on Electrical and Electronics Engineering (ELECO'09), Bursa, TÜRKİYE, 2009, pp.387-392.

[8] S. Özyön, C. Yaşar, "Gravitational Search Algorithm Applied to Fixed Head Hydrothermal Power System with Transmission Line Security Constraints," Energy, vol.155, pp.392-407, 2018. doi:10.1016/j.energy.2018.04.172

[9] M. S. Fakhar, S. A. R. Kashif, S. Liaquat, A. Rasool, S. Padmanaban, M. A. Iqbal, M. A. Baig, B. Khan, "Implementation of APSO and Improved APSO on Non-cascaded and Cascaded Short-term Hydrothermal Scheduling," IEEE Access, vol.9, pp.77784-77797, 2021. doi:10.1109/access.2021.3083528

[10] S. Fadıl, C. Yaşar, "A Pseudo Spot Price Algorithm Applied to Short-term Hydrothermal Scheduling Problem," Electric Power Components and Systems, vol.29, no.11, pp.112-119, 2010. doi:10.1080/153250001753239202

[11] A. E. Nezhad, S. Jowkar, T. T. Sabour, E. Rahimi, F. Ghanavati, F. Esmaeilnezhad, "A Short-term Wind-Hydrothermal Operational Framework in the Presence of Pumped-Hydro Storage," e-Prime - Advances in Electrical Engineering, Electronics and Energy, vol.8 (100577), pp.1-16, 2024. doi:10.1016/j.prime.2024.100577

[12] M. Basu, "A Simulated Annealing-based Goal-Attainment Method for Economic Emission Load Dispatch of Fixed Head Hydrothermal Power Systems," International Journal of Electrical Power & Energy Systems, vol.27, no.2, pp.147-153, 2004. doi:10.1016/j.ijepes.2004.09.004

[13] M. Basu, "Economic Environmental Dispatch of Fixed Head Hydrothermal Power Systems using Nondominated Sorting Genetic Algorithm-II," Applied Soft Computing, vol.11, no.3, pp.3046-3055, 2010. doi:10.1016/j.asoc.2010.12.005

[14] M. Basu, "Artificial Immune System for Fixed Head Hydrothermal Power System," Energy, vol.36, no.1, pp.606-612, 2010. doi:10.1016/j.energy.2010.09.057

[15] T. T. Nguyen, D. N. Vo, A. V. Truong, "Cuckoo Search Algorithm for Short-term Hydrothermal Scheduling," Applied Energy, vol.132, no.1, pp.276-287, 2014. doi:10.1016/j.apenergy.2014.07.017

[16] T. T. Nguyen, D. N. Vo, "Modified Cuckoo Search Algorithm for Short-term Hydrothermal Scheduling," International Journal of Electrical Power & Energy Systems, vol.65, pp.271-281, 2014. doi:10.1016/j.ijepes.2014.10.004

[17] N. Narang, J. S. Dhillon, D. P. Kothari, "Scheduling Short-term Hydrothermal Generation using Predator-prey Optimization Technique," Applied Soft Computing, vol.21, pp.298-308, 2014. doi:10.1016/j.asoc.2014.03.029

[18] A. Rasoulzadeh-akhijahani, B. Mohammadi-ivatloo, "Short-term Hydrothermal Generation Scheduling by a Modified Dynamic Neighborhood Learning based Particle Swarm Optimization," International Journal of Electrical Power & Energy Systems, vol.67, pp.350-367, 2014. doi:10.1016/j.ijepes.2014.12.011

[19] N. Gouthamkumar, V. Sharma, R. Naresh, "Disruption-based Gravitational Search Algorithm for Short-term Hydrothermal

Scheduling," Expert Systems with Applications, vol.42, no.20, pp.7000-7011, 2015. doi:10.1016/j.eswa.2015.05.017
[20] G. Chen, M. Gao, Z. Zhang, S. Li, "Hybridization of Chaotic Grey Wolf Optimizer and Dragonfly Algorithm for Short-term Hydrothermal Scheduling," IEEE Access, vol.8, pp.142996-143020, 2020. doi:10.1109/access.2020.3014114
[21] M.A. Almubaidin, A.N. Ahmed, L.M. Sidek, K.A.H. AL-Assifeh, A. El-Shafie, "Deriving Optimal Operation Rule for Reservoir System Using Enhanced Optimization Algorithms. Water Resources Management, vol.38, no.4, pp.1207-1223, 2024. doi:10.1007/s11269-010-9712-6
[22] M.S. Fakhar, S. Liaquat, S.A.R. Kashif, A. Rasool, M. Khizer, M.A. Iqbal, S. Padmanaban, "Conventional and metaheuristic optimization algorithms for solving short term hydrothermal scheduling problem: A review." IEEE Access, vol.9, pp.25993-26025, 2021. Doi:10.1109/access.2021.3055292
[23] S. Özyön, "Optimal Short-term Operation of Pumped-storage Power Plants with Differential Evolution Algorithm," Energy, vol.194(116866), pp.1-13, 2019. doi:10.1016/j.energy.2019.116866
[24] A.J. Wood, B.F. Wollenberg, G.B. Sheble, Power Generation Operation and Control, IEEE & Wiley, 2013, p.656.
[25] D. P. Kothari, J. S. Dhillon, Power System Optimization, PHI Learning Private Limited, 2007, p.732.
[26] S. Özyön, "Optimal Aktif Güç Dağıtımı için Karşıt Öğrenme Tabanlı Diferansiyel Gelişim Algoritmasi." Uludağ Üniversitesi Mühendislik Fakültesi Dergisi, vol.25, no.1, pp.231-246, 2020. doi:10.17482/uumfd.635957
[27] B. Durmuş, "Optimal Components Selection for Active Filter Design with Average Differential Evolution Algorithm," AEU - International Journal of Electronics and Communications, vol.94, pp.293-302, 2018. doi:10.1016/j.aeue.2018.07.021
[28] B. Durmuş, H. Temurtaş, S. Özyön, "The Design of Multiple Feedback Topology Chebyshev Low-pass Active Filter with Average Differential Evolution Algorithm," Neural Computing & Applications, vol.32, no.22, pp.17097-17113, 2020. doi:10.1007/s00521-020-04922-7
[29] S. Özyön, "The Solution of the Short-term Hydrothermal Coordination Problem by Improved Incremental Gravitational Search Algorithm," Electrical-Electronics Engineering, Ph.D. Thesis, Kütahya Dumlupınar University, Institute of Science and Technology, 2008.

BIOGRAPHIES

S. Özyön was born in Ayaş, Turkey, in 1981. He received a B.Sc. degree in electrical electronics engineering from Dumlupınar University, Kütahya, Turkey, in 2005 and an M.Sc. degree from the Department of Electrical Electronics Engineering, Dumlupınar University, Kütahya, Turkey, in 2009. He works as an Associate Professor in the Department of Electrical Electronics Engineering at Kütahya Dumlupınar University. His research areas include power systems analysis, economical operation of power systems, power distribution systems, renewable energy systems, and optimization techniques.

H. Temurtaş was born in Mersin, Turkey, in 1967. He received a B.Sc. degree in electrical electronics engineering from Middle East Technical University, Ankara, Turkey, in 1993; an M.Sc. degree from the Department of Electrical Electronics Engineering, Dumlupınar University, Kütahya, Turkey, in 1996; PhD degree in Electrical and Electronic Engineering from Sakarya University, Sakarya, Turkey in 2004. He works as an Associate Professor in the Department of Computer Engineering at Kütahya Dumlupınar University. His research areas include programming languages, control algorithms, and optimization techniques.

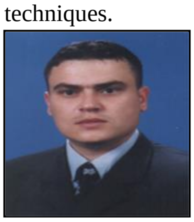

B. Durmuş was born in Pazaryeri, Turkey, in 1978. He received his B.Sc. and M.Sc. degrees in 2000 and 2003 from the Department of Electrical Electronics Engineering, Dumlupınar University, Kütahya, Turkey, respectively. He received a Ph.D. degree from Sakarya University. He works as an Associate Professor in the Department of Electrical Electronics Engineering at Kütahya Dumlupınar University. His areas of research include optimization techniques and computational intelligence.

C. Yaşar was born in Kütahya, Turkey, in 1958. He received the B.Sc.E.E. degree from the Yıldız Technical University, the M.Sc. E.E degree from the Anadolu University and Ph.D. degree from the Osmangazi University, Turkey, in 1980, 1988 and 1999, respectively. He works as a Professor at the Electrical and Electronics Engineering Department of Dumlupınar University, Turkey. His research interests include analysis of power systems, economical operation of power systems, power distribution systems, power system protection, and renewable energy systems.